JACS
JOURNAL OF THE AMERICAN CHEMICAL SOCIETY

ARTICLE

pubs.acs.org/JACS

Orbital Views of Molecular Conductance Perturbed by Anchor Units

Yuta Tsuji, Aleksandar Staykov, and Kazunari Yoshizawa*

Institute for Materials Chemistry and Engineering and International Research Center for Molecular Systems, Kyushu University, Fukuoka 819-0395, Japan

Supporting Information

ABSTRACT: Site-specific electron transport phenomena through benzene and benzenedithiol derivatives are discussed on the basis of a qualitative Hückel molecular orbital analysis for better understanding of the effect of anchoring sulfur atoms. A recent work for the orbital control of electron transport through aromatic hydrocarbons provided an important concept for the design of high-conductance connections of a molecule with anchoring atoms. In this work the origin of the frontier orbitals of benzenedithiol derivatives, the effect of the sulfur atoms on the orbitals and on the electron transport properties, and the applicability of the theoretical concept on aromatic hydrocarbons with the anchoring units are studied. The results demonstrate that the orbital view predictions are applicable to molecules perturbed by the anchoring units. The electron transport properties of benzene are found to be qualitatively consistent with those of benzenedithiol with respect to the site dependence. To verify the result of the Hückel molecular orbital calculations, fragment molecular orbital analyses with the extended Hückel molecular orbital theory and electron transport calculations with density functional theory are performed. Calculated results are in good agreement with the orbital interaction analysis. The phase, amplitude, and spatial distribution of the frontier orbitals play an essential role in the design of the electron transport properties through aromatic hydrocarbons.

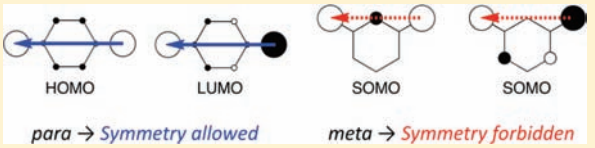

1. INTRODUCTION

During the last two decades studies of single-molecular electronic devices have gained great attention in nanoscale science and technology.[1−3] The variety of potential applications of molecular devices such as switches, rectifiers, and memories requires detailed understanding of the electron transport properties through a single molecule.[4−8] Recently, various π-conjugated molecular junctions have been investigated theoretically and experimentally (e.g., benzenedithiol (BDT),[2,4−7] polycyclic aromatic hydrocarbons,[5,6,9] and diarylethenes[7,10]). BDT is one of the most well-researched molecules, due to its simple geometrical and π-electronic structure. Several theoretical methods for calculation of the electron transport properties through single molecules have been developed, for instance, elastic-scattering Green's function method,[11,12] hopping models,[13,14] Lorentzian transmission model,[8,15] Lippmann−Schwinger method,[16,17] nonequilibrium Green's function (NEGF) method,[18−23] and free-electron network model.[24] These theoretical approaches yield a good inside view, which is required for better understanding the nature of electron transport through a single molecule and for design of single-molecular electronic devices. The NEGF method combined with density functional theory (NEGF-DFT) is the most common method used for description of the coherent electron transport, due to a proper treatment of the open-boundary conditions for a quantum system under a bias voltage, a fully atomistic treatment of the electrodes, and a self-consistent calculation of the charge density via the NEGF.[22] Qualitative views are of great importance for our understanding since qualitative methods take into account a few parameters and it is relatively easy to separate the most important contribution to the investigated phenomenon, which facilitates formulation of intuitive rules.[25]

Parallel to progress in theoretical approaches, rapid advances in fabrication techniques of single-molecular junctions have enabled us to obtain electron transport properties of individual molecules such as conductance, current−voltage characteristics, and shot noise.[1−8] After the pioneering measurement of the current−voltage characteristic of BDT located between two gold electrodes by Reed et al.,[26] various experimental techniques have been developed, for instance, mechanically controllable break junction (MCBJ),[26,27] scanning tunneling microscopy (STM),[28,29] atomic force microscopy (AFM),[30,31] mercury drop contact junction,[32,33] cross-wire junction,[34,35] and electromigration technique.[36,37] However, it is difficult to compare directly results observed with different methods since the conductance might be influenced by the binding sites (e.g., hollow site, bridge site, and on-top site)[38,39] and the number of molecules placed between the electrodes.[4] To settle these problems, the statistical approaches combined with MCBJ,[40−42] STM,[42−44] and AFM[45,46] have been developed and refined in recent years. In these methods, thousands of molecular junctions can be fabricated quickly and a large number of conductance traces and conductance histograms can be obtained, which allow us to determine the conductance of a single molecule with the most preferable contact geometry.[6,43,44] It is particularly worth noting that Song et al. recently reported direct electrostatic modulation of orbitals

Received: December 8, 2010
Published: March 24, 2011

dx.doi.org/10.1021/ja111021e | J. Am. Chem. Soc. 2011, 133, 5955–5965

in BDT using the electromigration technique.[47] This experimental result represents the realization of the molecular transistor and stimulates further investigations in the field of molecular electronics. Application of BDT to the molecular single-electron transistor has become an active area for theoretical research.[48]

In previous studies we proposed an orbital symmetry rule for electron transport properties of single molecules from analysis of Green's function in terms of the molecular orbital.[25,49−54] The orbital symmetry rule provides a powerful tool to predict the conductance through a single molecule. We demonstrated how to apply it on π-conjugated systems such as graphene sheets,[49−51] polycyclic aromatic hydrocarbons,[25,54] and diarylethenes.[52,53] Qualitative predictions based on the orbital symmetry rule with Hückel molecular orbital (HMO) theory are consistent with more quantitative DFT calculations.[25,52−54] The necessary preconditions for application of the orbital symmetry rule can be summarized as follows: (a) the coupling between the molecule and electrodes is weak, (b) there is electron−hole symmetry (pairing theorem)[55] in orbital energies and molecular orbital (MO) expansion coefficients, and (c) the Fermi level is located at the midgap of the highest occupied molecular orbital (HOMO) and the lowest unoccupied molecular orbital (LUMO).[25] According to Landauer's model, the conductance of a molecular junction composed of a molecule and two gold electrodes, in the limit of zero temperature and zero bias voltage, is written as follows[21]

$$g = \frac{2e^2}{h}T(E_F) \tag{1}$$

where $2e^2/h$ is the quantum conductance, T is the transmission probability, and E_F is the Fermi energy. We can calculate the transmission probability from eq 2[21]

$$T(E) = \mathrm{Tr}[\Gamma_L(E)\mathbf{G}^R(E)\Gamma_R(E)\mathbf{G}^A(E)] \tag{2}$$

where $\mathbf{G}^R$ ($\mathbf{G}^A$) and Γ_L (Γ_R) represent retarded (advanced) Green's function and the broadening function for the left (right) electrode, respectively. The broadening function is defined as $\Gamma_{L(R)} = i[\Sigma^R_{L(R)} - \Sigma^A_{L(R)}]$. $\Sigma^{R/A}_{L(R)}(E)$ is the self-energy matrix for the left (right) electrode and given by $\Sigma^{R/A}_{L(R)} = \tau^{\dagger}_{L(R)}\mathbf{g}^{R/A}_{L(R)}\tau_{L(R)}$, where $\mathbf{g}^{R/A}_{L(R)}$ is the Green's function of the left (right) electrode and $\tau_{L(R)}$ is the molecule−electrode interaction. We take only the nearest neighbor interactions between the electrode and the molecule into account. Retarded and advanced Green's functions are written as follows[56,57]

$$\mathbf{G}^{R/A}(E) = [\mathbf{I} - \mathbf{G}^{(0)R/A}(E)\Sigma^{R/A}(E)]^{-1}\mathbf{G}^{(0)R/A}(E) \tag{3}$$

where $\mathbf{I}$ is the unit matrix and $\mathbf{G}^{(0)R/A}$ is the zeroth Green's function, which is the Green's function of the molecule. The orbital symmetry rule is derived from the nature of the zeroth Green's function. According to eq 3, for a weak-coupling system, the Green's function is nearly proportional to the zeroth Green's function.[58,59] The conductance increases with an enhancement of the zeroth Green's function at the Fermi level. At the Fermi level the matrix elements of the zeroth Green's function, $G^{(0)R/A}_{rs}$, which describes the propagation of the tunneling electron from one side denoted with r to another side denoted with s through the orbitals in a noninteracting molecule, can be written as follows[60]

$$G^{(0)}_{rs}(E_F) = \sum_k \frac{C_{rk}C^*_{sk}}{E_F - \varepsilon_k \pm i\eta} \tag{4}$$

where C_{rk} is the kth MO coefficient at the rth atomic orbital (AO) in an orthogonal basis, ε_k is the kth MO energy, and η is an infinitesimal number determined by a relationship between the local density of states (LDOS) and the imaginary part of Green's function.[50,51] Equation 4 shows the correlation between the MOs and Green's function and makes it possible to predict the conductance from the MOs. In eq 4 the contributions from the HOMO and LUMO are written as follows

$$\frac{C_{r\mathrm{HOMO}}C^*_{s\mathrm{HOMO}}}{E_F - \varepsilon_{\mathrm{HOMO}} \pm i\eta} + \frac{C_{r\mathrm{LUMO}}C^*_{s\mathrm{LUMO}}}{E_F - \varepsilon_{\mathrm{LUMO}} \pm i\eta} \tag{5}$$

The contributions from these frontier orbitals are significant in the zeroth Green's function since the denominators of eq 5 are the smallest of all the terms of eq 4 because of the vicinity of the Fermi level. Subjacent and superjacent orbitals should not be important in electron transport since these orbitals are far away from the Fermi level and hardly contribute to the zeroth Green's function. It is described by the Fermi functions of the left and right electrodes, $f_L(E)$ and $f_R(E)$.[21] A level that is way below both electrochemical potentials of the left and right electrodes, μ_L and μ_R, will have $f_L(E) = f_R(E) = 1$ and will not contribute to the electron transport, just like a level that is way above both potentials μ_L and μ_R has $f_L(E) = f_R(E) = 0$. It is only when the level lies within a few k_BT of the potentials μ_L and μ_R that we have $f_L(E) \neq f_R(E)$ and an electron can move. The electron transport is thus a result of the difference in agenda between the left and the right electrodes. With attention to the reversal of the signs between the denominators in eq 5, we can derive the orbital symmetry rule, which requires enhancement of the contributions from the HOMO and LUMO. The orbital symmetry rule can be summarized as follows. To obtain effective electron transport through a single molecule, (a) two atoms in which the orbital amplitudes of the HOMO and LUMO are significant should be connected with electrodes and (b) two atoms in which the sign of the product of the MO expansion coefficients in the HOMO is different from that in the LUMO should be connected with electrodes.[25,49−54] One of the assumptions required for the orbital symmetry rule is that two gold electrodes have weak contact with the π-conjugated molecules, in which only the weak interactions between the $2p_z$ AO in carbon and the 6s AO in gold are considered.[49−51] However, in actual molecular junctions, the measured molecules are functionalized with two anchor groups that can chemically bind to the electrodes. Anchor groups play a crucial role in the reproducible formation of a molecular junction.[6] A wide range of anchor groups has been employed, for instance, thiol,[1−8] isocyanide,[61,62] pyridine,[43] selenide,[63,64] carboxylate,[65] phosphine,[66] amine,[67,68] and C_{60}.[69] The most widely used anchor group is thiol (−SH) because of the high binding affinity of the sulfur atom with the gold surface, where strong covalent Au−S bonds are formed.[1−8] Sulfur atoms should influence the spatial distribution of the frontier orbitals and the energy level alignment of the molecule. In this manuscript we consider the impact of the sulfur atoms on the orbital symmetry rule for the benzene molecule.

2. COMPUTATIONAL METHODS

2.1. Hückel Calculations. To look at the orbital symmetry rule for dithiol derivatives, we performed HMO calculations about *p*-BDT and *m*-BDT. The *o*-BDT is not appropriate for a molecular wire because the distance between the two sulfur atoms is too short. The parameters employed for sulfur atoms are $\alpha_S = \alpha_C$ and $\beta_{C-S} = 0.5\ \beta_{C-C}$, where

Scheme 1

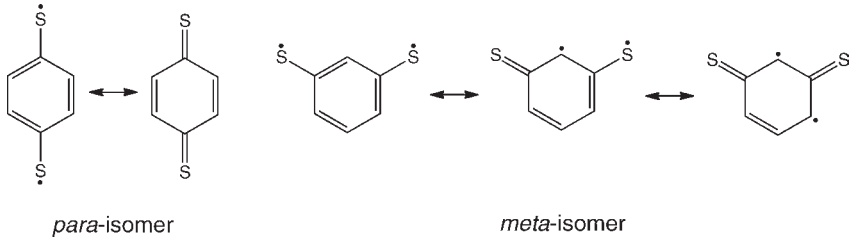

α and β are the Coulomb integral and resonance (transfer) integral, respectively. A wide range of methods to estimate α and β for heteroatoms is proposed.[70] We determined these values after a careful comparative review of various studies in the literature.[70−75] In the treatment of dithiol derivatives with HMO we considered six $2p_z$ orbitals of the carbon atoms and two $3p_z$ orbitals of the sulfur atoms. We assumed that one electron is allocated to each atom on the basis of the resonance structures shown in Scheme 1.

We performed the NEGF-HMO theory calculations to obtain the transmission spectra using the formalism given in previous papers.[25,49−54] The transmission spectra as a function of electron energy at zero bias provide qualitative and essential insights into the electron transport through BDT. In addition to the α and β values for the sulfur atoms, parameters for gold atoms are also required in the calculations. The parameters employed for gold atoms are $\beta_{Au-Au} = 0.6\beta_{C-C}$ and $\beta_{Au-S} = 0.28\beta_{C-C}$. The value of β_{Au-Au} was chosen from the literature,[25] while that of β_{Au-S} was estimated with the Wolfsberg−Helmholz approximation[76] within the framework of the extended Hückel molecular orbital (eHMO) method.[77] The distance between the sulfur and the gold atoms was set to be 2.31 Å for estimation of β_{Au-S}.

2.2. Extended Hückel Calculations. To obtain a better understanding of the effect of the sulfur atoms on the spatial distribution of the frontier orbitals and energy level alignment of benzene, we performed a fragment molecular orbital (FMO) analysis based on the eHMO method[78,79] using the YAeHMOP program.[80] The parameters used for the sulfur, carbon, and hydrogen atoms are S3s (H_{ii} = −20.00 eV, ζ = 2.122), S3p (H_{ii} = −11.00 eV, ζ = 1.827), C2s (H_{ii} = −21.40 eV, ζ = 1.625), C2p (H_{ii} = −11.40 eV, ζ = 1.625), and H1s (H_{ii} = −13.60 eV, ζ = 1.300), in which H_{ii} and ζ are the orbital energies and Slater exponents, respectively. For the eHMO calculations all C−C, C−H, and C−S bond distances were set to be 1.40, 1.09, and 1.79 Å, respectively.

2.3. DFT Calculations. We performed more quantitative electron transport calculations with the NEGF-DFT method using realistic molecular junction models to verify the efficacy of the qualitative calculations with HMO theory and eHMO theory. Prior to the electron transport calculations, geometry optimizations were performed with the Gaussian 03 program[81] at the B3LYP level of theory.[81−84] Models for geometry optimizations include one Au atom from the electrodes connected to each S atom. The 6-31G(d) basis set[85] was used for the C, H, and S atoms, and the LANL2DZ basis set[86] was used for the Au atoms. The electron transport calculations were performed for the zero-bias optimized geometries because studies in the literature[87,88] have shown that the applied electric field between the electrodes does not significantly alter the molecular geometry. The electron transport calculations were performed using the ATK 2008.10 program.[89] The method includes the full self-consistent field (SCF) treatment of molecular devices, in which the two gold electrodes are strongly coupled with BDT through Au−S chemical bonds. The effect of the external electric field on the electronic properties of the molecules is taken into account.[89] The adsorption site of BDT adopted in this study is the *fcc* 3-fold hollow site since a large number of studies[90−94] show that the hollow site

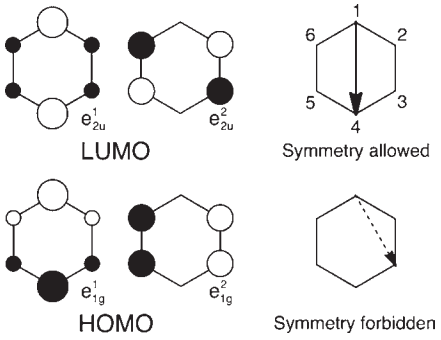

Figure 1. Frontier orbitals of benzene, symmetry-allowed, and symmetry-forbidden routes for electron transport.

bonding is more favorable in energy than other bonding manners. However, Ratner and co-workers[95] suggested that the interaction between the S atom and the electrode does not significantly influence the conductance. The electron transport calculation using the model optimized with three gold atoms from the Au(111) surface on each side of the molecule was performed, but the main features in the transmission spectrum were not affected significantly, as shown in the Supporting Information. The adsorption structure was determined by reference to the literature.[91] The semi-infinite left and right electrodes were modeled by two Au(111)-(3 × 3) surfaces (i.e., each layer includes nine Au atoms). The two probe models we used for the scattering region include 99 atoms from the Au(111) electrodes; six layers and five layers were used for the left and right electrodes, respectively. To save computational time, the single-ζ basis set (SZ) was used for the gold atoms and the double-ζ basis set with polarization (DZP) was used for all other atoms.[92] The exchange-correlation potential described by the Perdew−Zunger local density approximation (LDA-PZ) was employed.[96]

3. RESULTS AND DISCUSSION

The frontier orbitals of benzene calculated with HMO theory are shown in Figure 1. For connection 1−4 (para) the product of the MO coefficients on atoms 1 and 4 in the e^1_{1g} HOMO is different in sign from that in the e^1_{2u} LUMO and the orbital amplitudes of the HOMO and LUMO on those atoms are sufficiently large. It is not necessary to consider the e^2_{1g} HOMO and e^2_{2u} LUMO since the amplitudes on atoms 1 and 4 are zero. According to the orbital symmetry rule, we expect that the para connection should have high conductance and be described as symmetry allowed. For connection 1−3 (meta) the product of the MO coefficients on atoms 1 and 3 in the e^1_{1g} HOMO has the same sign as that in the e^1_{2u} LUMO. We do not need to consider the e^2_{1g} HOMO and e^2_{2u} LUMO since the amplitudes on atom 1 are zero. According to the orbital symmetry rule, we expect that

dx.doi.org/10.1021/ja111021e |*J. Am. Chem. Soc.* 2011, 133, 5955–5965

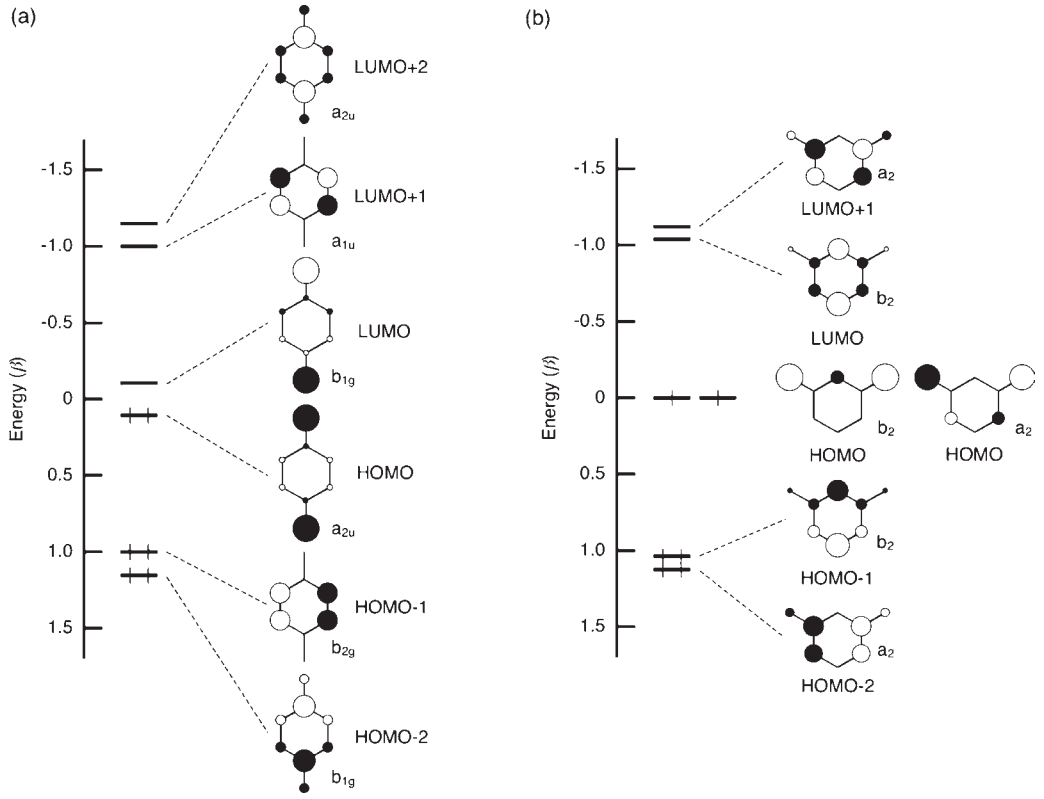

Figure 2. MO energy diagrams near the Fermi level and frontier orbitals of (a) *p*-BDT and (b) *m*-BDT calculated with HMO theory.

the meta connection should have low conductance and be described as symmetry forbidden.

The MO energy diagrams near the Fermi level and the frontier orbitals of benzene derivatives with two anchoring sulfur atoms calculated with HMO theory are shown in Figure 2. For *p*-BDT the product of the MO coefficients on the two anchoring sulfur atoms in the HOMO is different in sign from that in the LUMO and the orbital amplitudes of the HOMO and LUMO on those atoms are sufficiently large. Therefore, we expect that the electron transport through *p*-BDT is also symmetry allowed. The orbital symmetry rule holds true for the *p*-dithiol derivative. For *m*-BDT the b_2 HOMO and a_2 HOMO are degenerate, which is accidental degeneracy from the perspective of group theory. According to Scheme 1, the meta isomer belongs to the group of non-Kekulé molecules,[55] for which no classical structure can be drawn. Alternant hydrocarbons with n^* starred atoms and n unstarred atoms have $(n^* - n)$ nonbonding MOs (NBMOs), in which the conjugated atoms can be divided into two groups, starred and unstarred, in such a way that no two atoms of the same label are directly linked.[55] Longuet-Higgins also proposed a similar rule to predict the existence of NBMOs; alternant hydrocarbons have at least $N - 2T$ NBMOs, in which N denotes the number of carbon atoms in the conjugated system and T denotes the maximum number of double bonds occurring in any resonance structure.[97] The degeneracy of NBMOs is called topological degeneracy since it is determined by the sequence of carbon atoms forming the conjugated system.[98] We can regard the b_2 HOMO and a_2 HOMO as degenerate NBMO by expanding the concept of the topological degeneracy to the molecules with heteroatoms. The benzene derivatives with two organic radicals at the meta position such as *m*-quinodimethane[99] and *m*-quinone[100] have triplet ground states resulting from the 2-fold-degenerate orbitals consisting of the NBMOs.[98,101] In order to apply the orbital symmetry rule to the degenerate system, let us look back at the zeroth Green's function. In eq 4 the contributions from the b_2 HOMO and a_2 HOMO are written as follows

$$\frac{C_{rb_2\mathrm{HOMO}}C^*_{sb_2\mathrm{HOMO}}}{E_\mathrm{F} - \varepsilon_{b_2\mathrm{HOMO}} \pm i\eta} + \frac{C_{ra_2\mathrm{HOMO}}C^*_{sa_2\mathrm{HOMO}}}{E_\mathrm{F} - \varepsilon_{a_2\mathrm{HOMO}} \pm i\eta} \qquad (6)$$

The contributions from the b_2 HOMO and a_2 HOMO should be significant in the zeroth Green's function, for which the denominators in eq 6 are the smallest of all the terms in eq 4 because of the vicinity of the Fermi level. In eq 6, the values of the denominators are the same, due to the degeneracy of the b_2 HOMO and a_2 HOMO, and the sign of the $C_{rb_2\mathrm{HOMO}}C^*_{sb_2\mathrm{HOMO}}$ is different from the sign of the $C_{ra_2\mathrm{HOMO}}C^*_{sa_2\mathrm{HOMO}}$. Therefore cancellation occurs between the b_2 HOMO and a_2 HOMO. We expect that the electron transport through *m*-BDT is symmetry forbidden. The orbital symmetry rule holds true for the *m*-dithiol derivative. Thus, we can apply the orbital symmetry rule to the molecule with anchoring sulfur atoms just like the molecule without anchor units.

We show in Figure 3a and 3b computed transmission spectra for benzene and the benzene derivatives with two anchoring sulfur atoms calculated with HMO theory as a function of electron energy, respectively. The transmission probability at the Fermi level $(E = 0)$ is important since the conductance through a single molecule is proportional to the transmission probability at the Fermi level.[21] Figure 3a and 3b shows that at the Fermi level the para connections have high transmission probability whereas the meta connections have low transmission

dx.doi.org/10.1021/ja111021e | *J. Am. Chem. Soc.* 2011, 133, 5955–5965

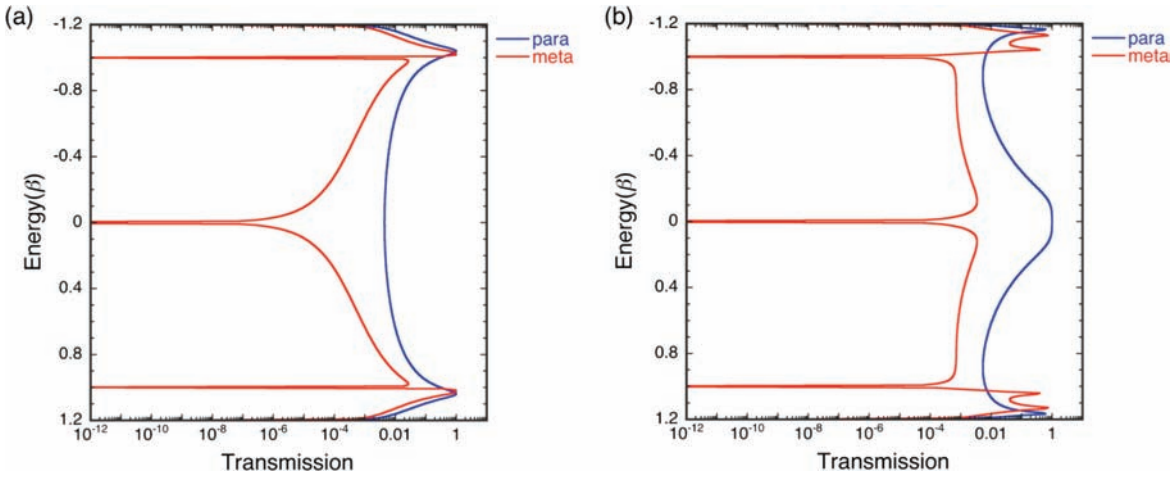

Figure 3. Computed transmission spectra of (a) benzene and (b) BDT calculated with HMO theory.

Scheme 2

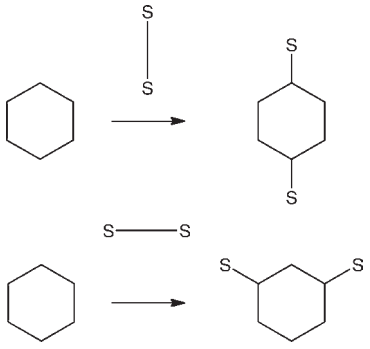

probability. These computational results are fully consistent with the qualitative analysis based on the frontier orbitals and other theoretical investigations based on the concept of quantum interference effects.[24,102−106] The two transmission dips at 1.0 β and −1.0 β in the meta connection can be explained based on the zeroth Green's function formalism. In the transmission dip at 1.0 β in Figure 3b, the HOMO−1 and HOMO−2 shown in Figure 2b play an important role. At E = 1.0 β the denominators of the zeroth Green's function are written as 1.0 β − $\varepsilon_{\mathrm{HOMO\text{-}1}}$ and 1.0 β − $\varepsilon_{\mathrm{HOMO\text{-}2}}$, respectively; 1.0 β − $\varepsilon_{\mathrm{HOMO\text{-}1}}$ is smaller than 1.0 β − $\varepsilon_{\mathrm{HOMO\text{-}2}}$, but the contributions from the HOMO−1 and HOMO−2 are equivalent since the amplitudes on the sulfur atoms in the HOMO−1 are also smaller than those in the HOMO−2. Since the signs of the denominators are the same, the difference in sign between $C_{r\mathrm{HOMO\text{-}1}}C^{*}_{s\mathrm{HOMO\text{-}1}}$ and $C_{r\mathrm{HOMO\text{-}2}}C^{*}_{s\mathrm{HOMO\text{-}2}}$ results in the cancellation of the contributions from the HOMO−1 and HOMO−2. However, in the case of the para connection, at E = 1.0 β the cancellation does not occur since only the HOMO−2 contributes to the zeroth Green's function, due to the absence of the amplitudes on the sulfur atoms in the HOMO−1. The transmission dip at −1.0 β is also explained by a similar procedure using LUMO and LUMO+1. The orbital symmetry rule based on the zeroth Green's function formalism is very useful for the discussion on the origin of transmission peaks and dips. Additionally, Figure 3b clearly shows that the transmission probability at the Fermi level is enhanced by introduction of the anchoring sulfur atoms since the sulfur atoms localize the π-electronic populations in the MOs near the Fermi level, as shown in Figure 2. The calculations including the anchoring units provide important understanding for the effect of those connecting groups on the conductance; however, the qualitative results remain unchanged.

In terms of orbital interactions one can reasonably characterize the difference between the electronic structures of *p*-BDT and *m*-BDT, which can be theoretically built up from the benzene molecule and a virtual disulfur molecule, as shown in Scheme 2. We thus apply the FMO method to better understand the electronic structures of *p*-BDT and *m*-BDT.

An orbital interaction diagram for *p*-BDT is shown in Figure 4, where the σ orbitals are neglected for clarity. Since the interaction between the two sulfur atoms is negligible because of the large distance between them, the π_u and π_g orbitals consisting of the $3p_z$ AOs of the sulfur atoms are almost degenerate. The e^1_{1g} HOMO of benzene and the π_g orbital of the disulfur molecule interact nicely at the connecting sites so that the in-phase combination b_{1g} orbital, the HOMO−2 of *p*-BDT, is stabilized and the out-of-phase counterpart b_{1g} orbital, the LUMO of *p*-BDT, is destabilized. Moreover, since the e^1_{2u} LUMO of benzene and the π_u orbital of the disulfur molecule also interact nicely, the in-phase combination a_{2u} orbital, the HOMO of *p*-BDT, is stabilized and the out-of-phase combination a_{2u} orbital, the LUMO+2 of *p*-BDT, is destabilized. As a consequence, the symmetry of the HOMO and LUMO of benzene is switched in *p*-BDT. However, the orbital symmetry rule is conserved in *p*-BDT since the combination of symmetry in the HOMO and LUMO remains unchanged. Additionally, it is essential to note that the HOMO−LUMO gap of *p*-BDT gets narrow as a result of the interaction between the benzene and the anchoring sulfur atoms.

We show in Figure 5 an orbital interaction diagram for *m*-BDT. The a_2 SOMO and b_2 SOMO are degenerate and satisfy the rule of topological degeneracy. In the case of *p*-BDT, the e^2_{1g} HOMO and e^2_{2u} LUMO of benzene transform to the b_{2g} HOMO−1 and a_{1u} LUMO+1 of *p*-BDT without interaction with the sulfur atoms. In the case of *m*-BDT, the energy levels of the b_2 HOMO−1 and b_2 LUMO of *m*-BDT, which correspond to the b_{2g} HOMO-1 and a_{1u} LUMO+1 of *p*-BDT, respectively, are shifted from the energy levels of the HOMO and LUMO of benzene. Therefore, the two SOMOs of *m*-BDT should be

dx.doi.org/10.1021/ja111021e |*J. Am. Chem. Soc.* 2011, 133, 5955–5965

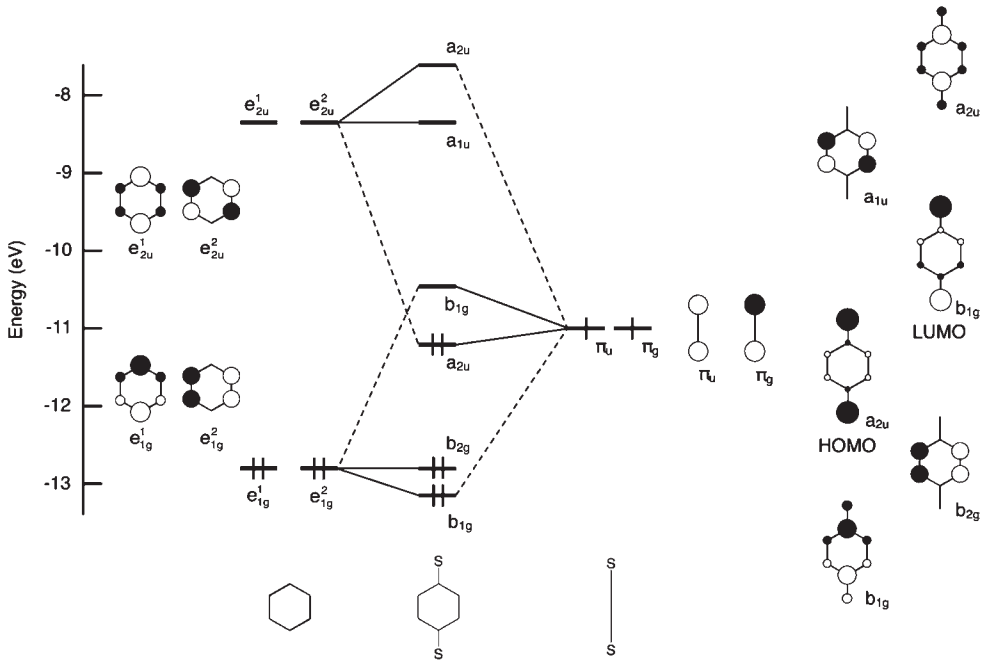

Figure 4. Orbital interaction diagram for *p*-BDT partitioned into benzene and a virtual disulfur molecule.

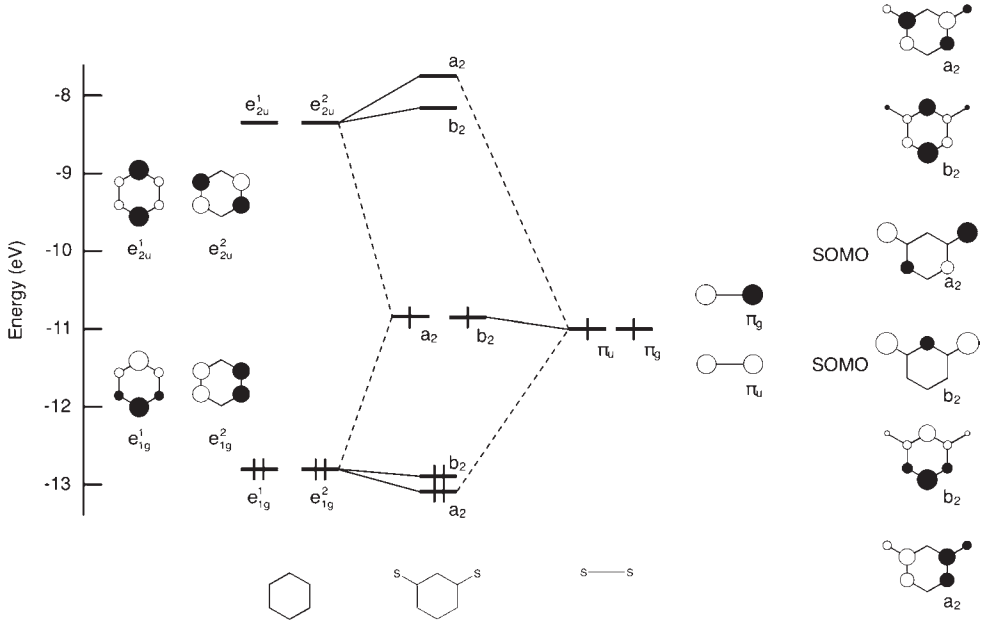

Figure 5. Orbital interaction diagram for *m*-BDT partitioned into benzene and a virtual disulfur molecule.

generated as a consequence of the contributions from the degenerate HOMOs and LUMOs of benzene and the two bonding and antibonding π orbitals of the disulfur molecule.

The extended validity that the orbital symmetry rule works in the model including the anchoring sulfur atoms lies in the energy level location of the disulfur molecule. The energy level of the two bonding and antibonding π orbitals of the disulfur molecule is the same as that of the 3p AO in sulfur, which is very close to that of the 2p AO in carbon. The ionization potentials of the 3p AO in sulfur and 2p AO in carbon are −11.0 and −11.4 eV, respectively. Since the two π orbitals of the disulfur molecule are located at the nearly midgap of the degenerate HOMOs and LUMOs of benzene, the two π orbitals of the disulfur molecule can almost equally interact with the degenerate HOMOs and LUMOs of benzene. The MOs perturbed by the anchoring sulfur atoms still keep the electron−hole symmetry, in particular combination of symmetry in the HOMO and LUMO.

The MO energy diagrams near the Fermi level of *p*-BDT and *m*-BDT calculated with HMO theory, shown in Figure 2, and the orbital interaction diagrams calculated with eHMO theory, shown in Figures 4 and 5, were verified by DFT calculations at the B3LYP level of theory. We show in Figure 6 MO energy diagrams

dx.doi.org/10.1021/ja111021e |*J. Am. Chem. Soc.* 2011, 133, 5955–5965

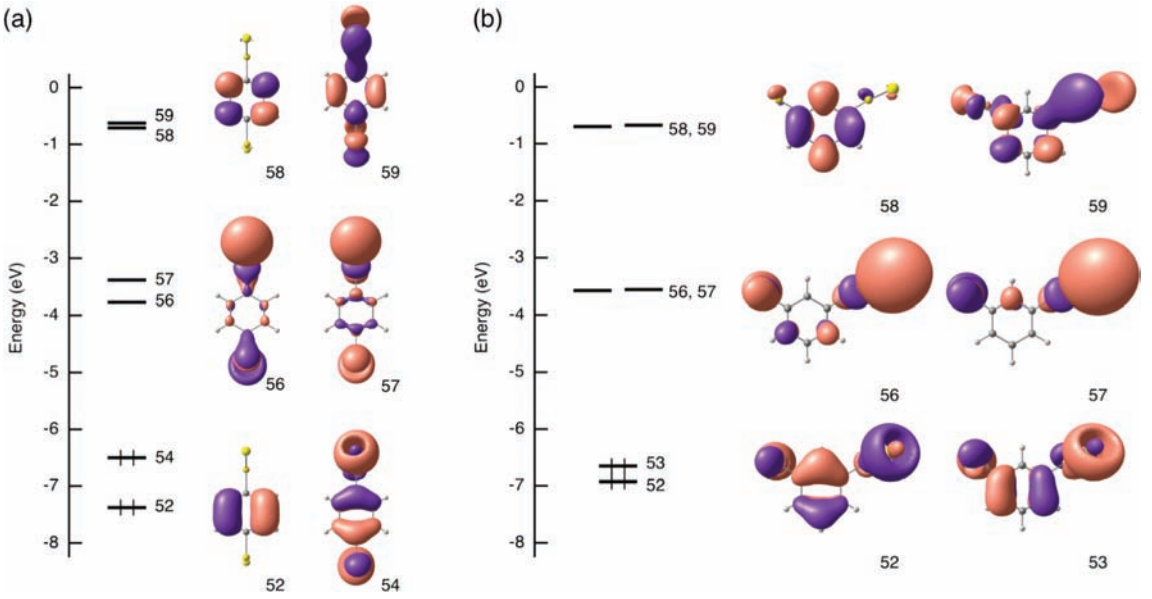

Figure 6. MO energy diagrams near the Fermi level and frontier orbital distributions of (a) *p*- and (b) *m*-benzene dithiolates with one gold atom attached to each sulfur atom calculated at the B3LYP level of theory.

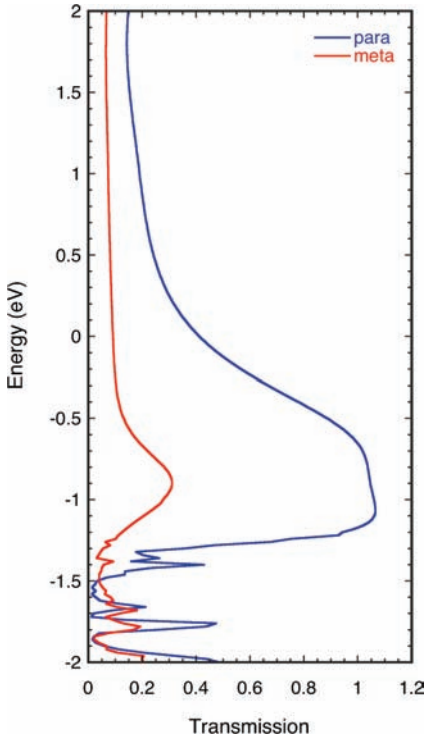

Figure 7. Computed transmission spectra of *p*- (blue) and *m*-benzene dithiolates (red) for zero bias with the NEGF-DFT method.

near the Fermi level and the frontier orbital distributions of the *p*- and *m*-benzene dithiolates with one gold atom attached to each sulfur atom. In this figure the σ-type orbitals, orbitals 53 and 55 for the para derivative and 54 and 55 for the meta derivative, are not shown because the π orbitals play the important role in the electron transport through π-conjugated molecules.

Although some energetically proximal orbitals flip places, the energy level alignments and orbital distributions are almost all consistent with the qualitative HMO and eHMO calculations. In particular, the meta derivative has 2-fold-degenerate NBMOs, as predicted by HMO calculations, while the para derivative does not have NBMOs. The existence or nonexistence of NBMOs in the vicinity of the Fermi level is closely related to the difference in the electron transport properties of the symmetry-allowed and symmetry-forbidden connections. A major difference between the HMO calculations and the DFT calculations is the location of the Fermi level. We assumed the Fermi level to lie just at the midgap of the HOMO and LUMO of benzene in the HMO calculations, whereas the location of the Fermi level is slightly lower in energy than the assumption.

We performed more quantitative calculations, which are closer to experimental models, using the NEGF-DFT method implemented in the ATK program. Computed transmission spectra are shown in Figure 7. The Fermi level is located at the origin of the energy ($E = 0$),[18,21] which was determined from DFT calculations of the bulk gold electrodes. The calculated transmission probability at the Fermi level for the para derivative is 0.41; on the other hand, that for the meta derivative is 0.09. This result is in good agreement with the qualitative expectations based on the frontier orbital analysis discussed earlier in this manuscript. In general, the conductance of molecules at low bias voltage decreases exponentially with an increase in molecular length L, which is described as $G = A \exp(-\gamma L)$, where A is a constant and γ is the decay constant.[4−6] Although the molecular length that corresponds to the distance between two sulfur atoms of the para derivative is 0.85 Å longer than that of the meta derivative, the conductance of the para derivative is about four times higher than that of the meta derivative. This result suggests that the factor of MOs is more important than the molecular length for the molecular conductance. The peaks in the transmission spectra can be ascribed to the MOs that provide the conduction channels. Both transmission spectra have broadened peaks around −1 eV, which results from multiple conduction channels, i.e., the HOMO and close-lying occupied MOs. This result indicates that the HOMO and close-lying occupied MOs are

dx.doi.org/10.1021/ja111021e |*J. Am. Chem. Soc.* 2011, 133, 5955–5965

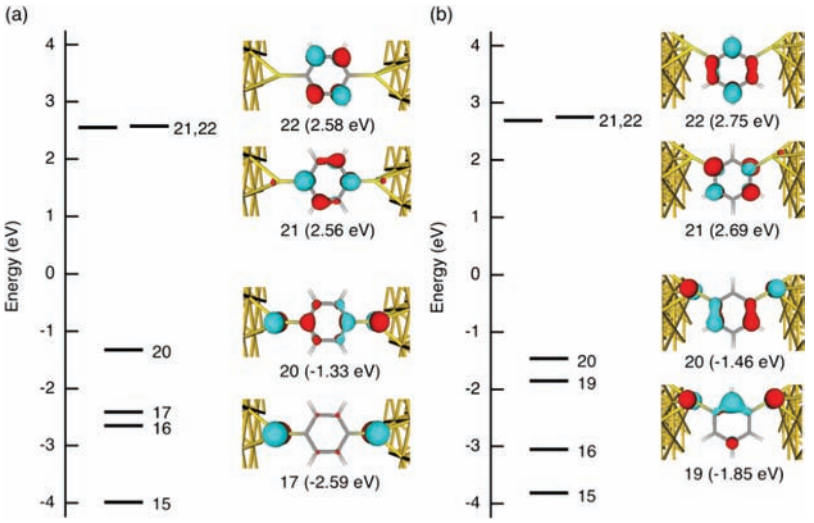

Figure 8. Molecular projected self-consistent Hamiltonian (MPSH) states of (a) *p*-BDT and (b) *m*-BDT contributing to the peaks in the transmission spectra.

closer to the Fermi level. We should pay more attention to the HOMO of BDT than the LUMO in interpreting the results of the more quantitative NEGF-DFT calculations.

The transmission peaks are related to the molecular orbitals of *p*- and *m*-BDT. The spatial distribution of the frontier orbitals for *p*- and *m*-BDT is affected by the electrodes. To obtain these affected orbitals, an effective method has been proposed, where the self-consistent Hamiltonian of the molecular junction is projected onto the molecule, and this molecular projected self-consistent Hamiltonian (MPSH) matrix is diagonalized.[20,89,107] The MPSH states are the eigenstates of the molecule within the two-probe environment and do not include the self-energies of the electrodes. The complex portion of the self-energy broadens the transmission peaks, while the real part will give a shift of the transmission peaks, relative to the MPSH states. Therefore, the transmission peaks and the MPSH energies do not always coincide. MPSH analysis helps us to qualitatively understand the origin of the transmission peaks. We show in Figure 8 MPSH states and spatial distributions of the four closest orbitals to the Fermi level for *p*- and *m*-BDT. In this figure MPSH states composed of the σ-type orbitals, states 18 and 19 for *p*-BDT and 17 and 18 for *m*-BDT, are not shown and orbitals extended to the electrodes are excluded for clarity. The energy level alignments and orbital distributions of the MPSH states are almost all consistent with the results of the qualitative HMO, eHMO, and higher-level DFT calculations for the insulated molecules. MPSH states 21 and 22 for both *p*- and *m*-BDT do not make significant contributions to transmission peaks since only MPSH states that are spatially delocalized throughout the scattering region and possess significant values on the terminating anchor atoms, which results in good overlap between the molecule and electrodes, will give peaks in the transmission spectra. MPSH states 17 and 20 for *p*-BDT and 19 and 20 for *m*-BDT play a crucial role in the electron transport through BDT molecules, and these orbitals are responsible for the transmission peaks around −1 eV. In *m*-BDT the energy difference between the MPSH states 19 and 20 is 0.39 eV, and these orbitals are not exactly degenerate because of the strong coupling between the molecule and the electrodes. In eq 4 the contributions from MPSH states 17 and 20 for *p*-BDT and 19 and 20 for *m*-BDT are

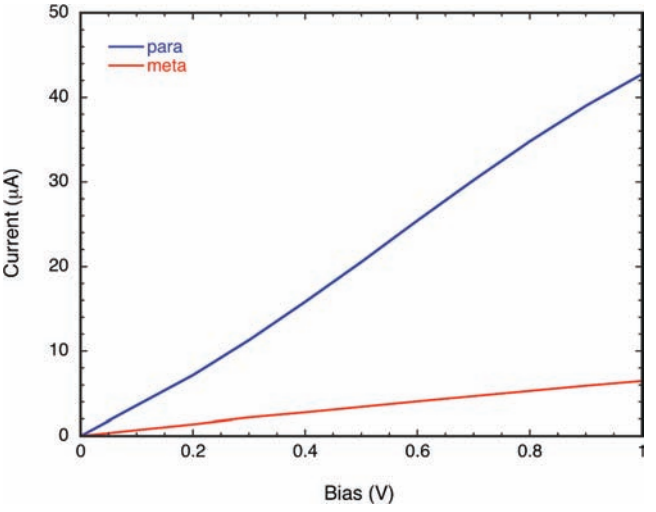

Figure 9. Computed *I*−*V* curves of *p*- (blue) and *m*-benzene dithiolates (red) with the NEGF-DFT method.

written as follows

$$\frac{C_{r17(19)}C^*_{s17(19)}}{E_F - \varepsilon_{17(19)} \pm i\eta} + \frac{C_{r20}C^*_{s20}}{E_F - \varepsilon_{20} \pm i\eta} \quad (7)$$

In eq 7, the signs of the denominators are the same and the signs of the numerators are different in both *p*- and *m*-BDT. In *p*-BDT the energy difference between MPSH states 17 and 20 is 1.26 eV, which is nearly three times larger than that in *m*-BDT. $E_F - \varepsilon_{20}$ = 1.33 eV is much smaller than $E_F - \varepsilon_{17}$ = 2.59 eV in *p*-BDT, whereas $E_F - \varepsilon_{20}$ = 1.46 eV is not much smaller than $E_F - \varepsilon_{19}$ = 1.85 eV in *m*-BDT. According to eq 7, in *p*-BDT at the Fermi level MPSH state 20 mainly contributes to the transmission probability whereas in *m*-BDT at the Fermi level both MPSH states 20 and 19 contribute to the transmission probability. Therefore, the smaller transmission probability at the Fermi level in *m*-BDT compared to that in *p*-BDT is attributed to the partial cancellation of the two nearly degenerate transport channels, MPSH states 20 and 19. The difference in conductance

behavior between *p*- and *m*-BDT results from the difference in energy splitting between states 17 and 20 for *p*-BDT and 19 and 20 for *m*-BDT.

Computed *I*−*V* curves of *p*-BDT and *m*-BDT with the NEGF-DFT method are shown in Figure 9. This figure describes the difference in the electron transport properties between the para derivative and the meta derivative. The current ratio of the para connection and meta connection is 1 order of magnitude. The computed *I*−*V* curves clearly show good agreement between the qualitative predictions based on the phase and amplitudes of the frontier orbitals within the HMO method and the quantitative calculations with the DFT method.

4. SUMMARY AND CONCLUSIONS

Our recent work for the orbital control of electron transport through aromatic hydrocarbons[25] provided an important concept to design high-conductance nanoelectronic devices. The theoretical framework was developed for weak interactions between the hydrocarbons and the electrodes; however, calculations with more quantitative methods have shown that the predictions hold true for realistic junctions that include anchoring units between the molecules and the electrodes. In this work we investigated the origin of the frontier orbitals of BDT derivatives, the effect of the sulfur atoms on the orbitals and on the electron transport properties, and the applicability of the theoretical concept on aromatic hydrocarbons with anchoring units. Our results clearly demonstrate that the orbital view predictions hold true for molecules perturbed by the anchoring units. The conductance through *p*-BDT is expected to be symmetry allowed, whereas that of *m*-BDT is expected to be symmetry forbidden. The difference between the symmetry-allowed and symmetry-forbidden connections was characterized from the detailed orbital interaction analysis within eHMO theory, i.e., FMO analysis. The MO energy diagrams and orbital interaction diagrams near the Fermi level of *p*-BDT and *m*-BDT were verified by DFT calculations at the B3LYP level of theory. The energy level alignments and orbital distributions are consistent with the qualitative HMO and eHMO calculations. We compared the qualitative expectations based on the frontier orbitals with HMO theory and eHMO theory with the NEGF-DFT calculations using more realistic two-probe models. The qualitative frontier orbital analysis is fully consistent with the quantitative NEGF-DFT calculation. The orbital symmetry rule is applicable to site-dependent electron transport properties of molecules with anchoring sulfur atoms. The results are not unique to the benzene and BDT derivatives. We obtained similar results for naphthalene and naphthalenedithiol derivatives. In this manuscript we considered a sulfur-anchoring system. The orbital symmetry rule will be expanded to other anchoring systems in our future work. Since essential orbital natures are very similar among Hückel, extended Hückel, Hartree−Fock, and DFT calculations, especially regarding symmetry,[108] the qualitative orbital views are useful in rationalizing the electron transport phenomena in molecular junctions.

■ ASSOCIATED CONTENT

Supporting Information. Atomic Cartesian coordinates for the optimized geometries of all investigated structures and complete ref 81. This material is available free of charge via the Internet at http://pubs.acs.org.

■ AUTHOR INFORMATION

Corresponding Author
kazunari@ms.ifoc.kyushu-u.ac.jp

■ ACKNOWLEDGMENT

K.Y. thanks Grants-in-Aid for Scientific Research (Nos. 18GS0207 and 22245028) from the Japan Society for the Promotion of Science (JSPS) and the Ministry of Education, Culture, Sports, Science and Technology of Japan (MEXT), the Kyushu University Global COE Project, the Nanotechnology Support Project, the MEXT Project of Integrated Research on Chemical Synthesis, and CREST of the Japan Science and Technology Cooperation.

■ REFERENCES

(1) Carroll, R. L.; Gorman, C. B. *Angew. Chem., Int. Ed.* **2002**, *41*, 4378.
(2) Nitzan, A.; Ratner, M. A. *Sience* **2003**, *300*, 1384.
(3) In *Introducing Molecular Electronics*; Cuniberti, G., Fagas, G., Richter, K., Eds.; Springer-Verlag: Berlin, Heidelberg, 2005.
(4) Salomon, A.; Cahen, D.; Lindsay, S.; Tomfohr, J.; Engelkes, V. B.; Frisbie, C. D. *Adv. Mater.* **2003**, *15*, 1881.
(5) Tao, N. J. *Nat. Nanotechnol.* **2006**, *1*, 173.
(6) Chen, F.; Tao, N. J. *Acc. Chem. Res.* **2009**, *42*, 429.
(7) van der Molen, S. J.; Liljeroth, P. *J. Phys.: Condens. Matter* **2010**, *22*, 133001.
(8) Malen, J. A.; Yee, S. K.; Majumdar, A.; Segalman, R. A. *Chem. Phys. Lett.* **2010**, *491*, 109.
(9) Müllen, K.; Rabe, J. P. *Acc. Chem. Res.* **2008**, *41*, 511.
(10) Matsuda, K.; Irie, M. *J. Photochem. Photobiol., C* **2004**, *5*, 169.
(11) Economou, E. N. *Green's Functions in Quantum Physics*; Springer: Berlin, 1990.
(12) Wang, C.-K.; Fu, Y.; Luo, Y. *Phys. Chem. Chem. Phys.* **2001**, *3*, 5017.
(13) Petrov, E. G.; Hänggi, P. *Phys. Rev. Lett.* **2001**, *86*, 2862.
(14) Hettler, M. H.; Schoeller, H.; Wenzel, W. *Europhys. Lett.* **2002**, *57*, 571.
(15) Paulsson, M.; Datta, S. *Phys. Rev. B* **2003**, *67*, 241403.
(16) Kobayashi, N.; Aono, M.; Tsukada, M. *Phys Rev. B* **2001**, *64*, 121402.
(17) Nara, J.; Geng, W. T.; Kino, H.; Kobayashi, N.; Ohno, T. *J. Chem. Phys.* **2004**, *121*, 6485.
(18) Xue, Y.; Datta, S.; Ratner, M. A. *J. Chem. Phys.* **2001**, *115*, 4292.
(19) Brandbyge, M.; Mozos, J.-L.; Ordejón, P.; Taylor, J.; Stokbro, K. *Phys. Rev. B* **2002**, *65*, 165401.
(20) Stokbro, K.; Taylor, J.; Brandbyge, M.; Mozos, J.-L.; Ordejón, P. *Comput. Mater. Sci.* **2003**, *27*, 151.
(21) Datta, S. *Quantum Transport: Atom to Transistor*; Cambridge University Press: Cambridge, 2005.
(22) In *Molecular and Nano Electronics: Analysis, Design and Simulation*; Seminario, J. M., Ed.; Elsevier: Amsterdam, 2006; Vol. 17.
(23) Stokbro, K. *J. Phys.: Condens. Matter* **2008**, *20*, 064216.
(24) Hsu, L.-Y.; Jin, B.-Y. *Chem. Phys.* **2009**, *355*, 177.
(25) Yoshizawa, K.; Tada, T.; Staykov, A. *J. Am. Chem. Soc.* **2008**, *130*, 9406.
(26) Reed, M. A.; Zhou, C.; Muller, C. J.; Burgin, T. P.; Tour, J. M. *Science* **1997**, *278*, 252.
(27) Dulić, D.; van der Molen, S. J.; Kudernac, T.; Jonkman, H. T.; de Jong, J. J. D.; Bowden, T. N.; van Esch, J.; Feringa, B. L.; van Wees, B. J. *Phys. Rev. Lett.* **2003**, *91*, 207402.
(28) Donhauser, Z. J.; Mantooth, B. A.; Kelly, K. F.; Bumm, L. A.; Monnell, J. D.; Stapleton, J. J.; Price, D. W., Jr.; Rawlett, A. M.; Allara, D. L.; Tour, J. M.; Weiss, P. S. *Science* **2001**, *292*, 2303.

(29) Moth-Poulsen, K.; Patrone, L.; Stuhr-Hansen, N.; Christensen, J. B.; Bourgoin, J.-P.; Bjørnholm, T. *Nano Lett.* **2005**, *5*, 783.
(30) Wold, D. J.; Haag, R.; Rampi, M. A.; Frisbie, C. D. *J. Phys. Chem. B* **2002**, *106*, 2813.
(31) Ishida, T.; Mizutani, W.; Aya, Y.; Ogiso, H.; Sasaki, S.; Tokumoto, H. *J. Phys. Chem. B* **2002**, *106*, 5886.
(32) Holmlin, R. E.; Ismagilov, R. F.; Haag, R.; Mujica, V.; Ratner, M. A.; Rampi, M. A.; Whitesides, G. M. *Angew. Chem., Int. Ed.* **2001**, *40*, 2316.
(33) Holmlin, R. E.; Haag, R.; Chabinyc, M. L.; Ismagilov, R. F.; Cohen, A. E.; Terfort, A.; Rampi, M. A.; Whitesides, G. M. *J. Am. Chem. Soc.* **2001**, *123*, 5075.
(34) Kushmerick, J. G.; Holt, D. B.; Pollack, S. K.; Ratner, M. A.; Yang, J. C.; Schull, T. L.; Naciri, J.; Moore, M. H.; Shashidhar, R. *J. Am. Chem. Soc.* **2002**, *124*, 10654.
(35) Kushmerick, J. G.; Holt, D. B.; Yang, J. C.; Naciri, J.; Moore, M. H.; Shashidhar, R. *Phys. Rev. Lett.* **2002**, *89*, 086802.
(36) Strachan, D. R.; Smith, D. E.; Johnston, D. E.; Park, T.-H.; Therien, M. J.; Bonnell, D. A.; Johnson, A. T. *Appl. Phys. Lett.* **2005**, *86*, 043109.
(37) Osorio, E. A.; O'Neill, K.; Wegewijs, M.; Stuhr-Hansen, N.; Paaske, J.; Bjørnholm, T.; van der Zant, H. S. J. *Nano Lett.* **2007**, *7*, 3336.
(38) Bratkovsky, A. M.; Kornilovitch, P. E. *Phys. Rev. B.* **2003**, *67*, 115307.
(39) Nara, J.; Kino, H.; Kobayashi, N.; Tsukada, M.; Ohno, T. *Thin Solid Films* **2003**, *438*−*439*, 221.
(40) Dulić, D.; Tuukkanen, S.; Chung, C. L.; Isambert, A.; Lavie, P.; Filoramo, A. *Nanotechnology* **2009**, *20*, 115502.
(41) Tsutsui, M.; Taniguchi, M.; Kawai, T. *J. Am. Chem. Soc.* **2009**, *131*, 10552.
(42) Kiguchi, M.; Murakoshi, K. *Thin Solid Films* **2009**, *518*, 466.
(43) Xu, B. Q.; Tao, N. J. *Science* **2003**, *301*, 1221.
(44) Xiao, X. Y.; Xu, B. Q.; Tao, N. J. *Nano Lett.* **2004**, *4*, 267.
(45) Xu, B. Q.; Xiao, X. Y.; Tao, N. J. *J. Am. Chem. Soc.* **2003**, *125*, 16164.
(46) Huang, Z. F.; Xu, B. Q.; Chen, Y. C.; Di Ventra, M.; Tao, N. J. *Nano Lett.* **2006**, *6*, 1240.
(47) Song, H.; Kim, Y.; Jang, Y. H.; Jeong, H.; Reed, M. A.; Lee, T. *Nature* **2009**, *462*, 1039.
(48) Stokbro, K. *J. Phys. Chem. C* **2010**, *114*, 20461.
(49) Tada, T.; Yoshizawa, K. *ChemPhysChem* **2002**, *3*, 1035.
(50) Tada, T.; Yoshizawa, K. *J. Phys. Chem. B* **2003**, *107*, 8789.
(51) Tada, T.; Yoshizawa, K. *J. Phys. Chem. B* **2004**, *108*, 7565.
(52) Tsuji., Y.; Staykov, A.; Yoshizawa, K. *Thin Solid Films* **2009**, *518*, 444.
(53) Tsuji., Y.; Staykov, A.; Yoshizawa, K. *J. Phys. Chem. C* **2009**, *113*, 21477.
(54) Li, X.; Staykov, A.; Yoshizawa, K. *J. Phys. Chem. C* **2010**, *114*, 9997.
(55) Dewar, M. J. S. *The Molecular Orbital Theory of Organic Chemistry*; McGraw-Hill: New York, 1969.
(56) Kondo, M.; Tada, T.; Yoshizawa, K. *J. Phys. Chem. A* **2004**, *108*, 9143.
(57) Tada, T.; Nozaki, D.; Kondo, M.; Hamayama, S.; Yoshizawa, K. *J. Am. Chem. Soc.* **2004**, *126*, 14182.
(58) Caroli, C.; Combescot, R.; Nozieres, P.; Saint-James, D. *J. Phys. C* **1971**, *4*, 916.
(59) Combescot, R. *J. Phys. C* **1971**, *4*, 2611.
(60) Priyadarshy, S.; Skourtis, S. S.; Risser, S. M.; Beratan, D. N. *J. Chem. Phys.* **1996**, *104*, 9473.
(61) Beebe, J. M.; Engelkes, V. B.; Miller, L. L.; Frisbie, C. D. *J. Am. Chem. Soc.* **2002**, *124*, 11268.
(62) Kiguchi, M.; Miura, S.; Hara, K.; Sawamura, M.; Murakoshi, K. *Appl. Phys. Lett.* **2006**, *89*, 213104.
(63) Patrone, L.; Palacin, S.; Bourgoin, J. P. *Appl. Surf. Sci.* **2003**, *212*−*213*, 446.
(64) Patrone, L.; Palacin, S.; Charlier, J.; Armand, F.; Bourgoin, J. P.; Tang, H.; Gauthier, S. *Phys. Rev. Lett.* **2003**, *91*, 096802.
(65) Chen, F.; Li, X.; Hihath, J.; Huang, Z.; Tao, N. *J. Am. Chem. Soc.* **2006**, *128*, 15874.
(66) Park, Y. S.; Whalley, A. C.; Kamenetska, M.; Steigerwald, M. L.; Hybertsen, M. S.; Nuckolls, C.; Venkataraman, L. *J. Am. Chem. Soc.* **2007**, *129*, 15768.
(67) Quek, S. Y.; Venkataraman, L.; Choi, H. J.; Louie, S. G.; Hybertsen, M. S.; Neaton, J. B. *Nano Lett.* **2007**, *7*, 3477.
(68) Kiguchi, M.; Miura, S.; Hara, K.; Sawamura, M.; Murakoshi, K. *Appl. Phys. Lett.* **2007**, *91*, 053110.
(69) Martin, C. A.; Ding, D.; Sørensen, J. K.; Bjørnholm, T.; van Ruitenbeek, J. M.; van der Zant, H. S. J. *J. Am. Chem. Soc.* **2008**, *130*, 13198.
(70) Streitwieser, A., Jr. *Molecular Orbital Theory for Organic Chemists*; John Wiley & Sons: New York, 1961.
(71) Metzger, J.; Pullman, A. *Compt. Rend.* **1948**, *226*, 1613.
(72) Longuet-Higgins, H. C. *Trans. Faraday Soc.* **1949**, *45*, 173.
(73) Nagakura, S.; Hosoya, T. *Bull. Chem. Soc. Jpn.* **1952**, *25*, 179.
(74) Kreevoy, M. M. *J. Am. Chem. Soc.* **1958**, *80*, 5543.
(75) Pullman, B.; Pullman, A. *Rev. Mod. Phys.* **1960**, *32*, 428.
(76) Wolfsberg, M.; Helmholz, L. *J. Chem. Phys.* **1952**, *20*, 837.
(77) Hoffmann, R. *J. Chem. Phys.* **1963**, *39*, 1397.
(78) Albright, T. A.; Burdett, J. K.; Whangbo, M.-H. *Orbital Interactions in Chemistry*; Wiley: New York, 1985.
(79) Yoshizawa, K.; Yahara, K.; Tanaka, K.; Yamabe, T. *J. Phys. Chem. B* **1998**, *102*, 498.
(80) Landrum, G. *YAeHMOP (Yet Another Extended Hückel Molecular Orbital Package)*; Cornell University: Ithaca, NY, 1995.
(81) Frisch, M. J.; et al. *Gaussian 03*, revision B.03; Gaussian, Inc.: Wallingford, CT, 2004.
(82) Becke, A. *J. Chem. Phys.* **1993**, *98*, 5648.
(83) Lee, C.; Yang, W.; Parr, R. *Phys. Rev. B* **1988**, *37*, 785.
(84) Vosko, S.; Wilk, L.; Nusair, M. *Can. J. Phys.* **1980**, *58*, 1200.
(85) Krishnan, R.; Binkley, J.; Seeger, R.; Pople, J. A. *J. Chem. Phys.* **1980**, *72*, 650.
(86) Hay, P.; Wadt, W. *J. Chem. Phys.* **1985**, *82*, 270.
(87) Yin, X.; Li, Y.; Zhang, Y.; Li, P.; Zhao, J. *Chem. Phys. Lett.* **2006**, *422*, 111.
(88) Li, Y.; Zhao, J.; Yin, X.; Yin, G. *J. Phys. Chem. A* **2006**, *110*, 11130.
(89) *ATK*, version 2008.10; QuantumWise: Copenhagen, Denmark, 2008; www.quantumwise.com.
(90) Grönbeck, H.; Curioni, A.; Andreoni, W. *J. Am. Chem. Soc.* **2000**, *122*, 3839.
(91) Tachibana, M.; Yoshizawa, K.; Ogawa, A.; Fujimoto, H.; Hoffmann, R. *J. Phys. Chem. B* **2002**, *106*, 12727.
(92) Bauschlicher, C. W.; Ricca, A. *Chem. Phys. Lett.* **2003**, *367*, 90.
(93) Nara, J.; Higai, S.; Morikawa, Y.; Ohno, T. *J. Chem. Phys.* **2004**, *120*, 6705.
(94) Cometto, F.; Paredes-Olivera, P.; Macagno, V.; Patrito, E. *J. Phys. Chem. B* **2005**, *109*, 21737.
(95) Yaliraki, S. N.; Kemp, M.; Ratner, M. A. *J. Am. Chem. Soc.* **1999**, *121*, 3428.
(96) Perdew, J.; Zunger, A. *Phys. Rev. B* **1981**, *23*, 5048.
(97) Longuet-Higgins, H. C. *J. Chem. Phys.* **1950**, *18*, 265.
(98) Itoh, K. *Pure Appl. Chem.* **1978**, *50*, 1251.
(99) Kato, S.; Morokuma, K.; Feller, D.; Davidson, E. R.; Borden, W. T. *J. Am. Chem. Soc.* **1983**, *105*, 1791.
(100) Fort, R. C.; Getty, S. J.; Hrovat, D. A.; Lahti, P. M.; Borden, W. T. *J. Am. Chem. Soc.* **1992**, *114*, 7549.
(101) Ovchinnikov, A. A. *Theoret. Chim. Acta* **1978**, *47*, 297.
(102) Maiti, S. K. *Phys. Lett. A* **2007**, *366*, 114.
(103) Solomon, G. C.; Andrews, D. Q.; Hansen, T.; Goldsmith, R. H.; Wasielewski, M. R.; Van Duyne, R. P.; Ratner, M. A. *J. Chem. Phys.* **2008**, *129*, 054701.
(104) Ke, S.-H.; Yang, W.; Baranger, H. U. *Nano Lett.* **2008**, *8*, 3257.
(105) Liu, H.; Ni, W.; Zhao, J.; Wang, N.; Guo, Y.; Taketsugu, T.; Kiguchi, M.; Murakoshi, K. *J. Chem. Phys.* **2009**, *130*, 244501.

(106) Hansen, T.; Solomon, G. C.; Andrews, D. Q.; Ratner, M. A. *J. Chem. Phys.* **2009**, *131*, 194704.
(107) Staykov, A.; Nozaki, D.; Yoshizawa, K. *J. Phys. Chem. C* **2007**, *111*, 11699.
(108) Stowasser, R.; Hoffmann, R. *J. Am. Chem. Soc.* **1999**, *121*, 3414.